Electronic, magnetic, and optical properties of Gd monopnictides: An LDA+U study

Dipta Bhanu Ghosh, Molly De, and S. K. De
Department of Materials Science, Indian Association for the Cultivation of Science, Jadavpur, Kolkata 700 032, India
(Received 10 November 2004; revised manuscript received 30 March 2005; published 25 July 2005)

The electronic structure calculation of Gd monopnictides has been performed by the linear muffin-tin orbital method. The correlation effects among the f states are considered in the local density approximation. The rigid shifts in the 5d and 4f states are required to obtain the correct electronic structure of Gd monopnictides. The calculated magnetic moment is very close to the atomic value. Reflectivity calculations reveal a plasma edge effect in GdP, GdAs, and GdSb and agree well with the experimental results. The resonance like structures in the Kerr rotation and the ellipticity spectrum are found. The deep plasma minimum results in a large Kerr rotation in GdP, GdAs, and GdSb.

DOI: 10.1103/PhysRevB.72.045140 PACS number(s): 78.20.Ls

I. INTRODUCTION

The rare earth (RE) monopnictides exhibit a rich variety in their physical properties. The electronic, magnetic, and magneto-optical properties of such a system primarily depend on the behavior of f electrons under the influence of the ligand. The degree of localization and the position of f bands depend on the rare earth element and also on its chemical environment. Gadolinium is at the center of the lanthanide series and has a half-filled 4f orbital configuration. Hence, it is to be expected that the 4f electrons will be strongly localized and magnetic properties will be dominated by the exchange interaction. Gd monopnictides (GdX,X=N,P,As,Sb,Bi) are known to exhibit unusual electric[1] and magnetic[2,3] phenomena. GdN is a controversial semimetallic compound, which might be a very small-gap semiconductor. Other monopnictides, GdP to GdBi are semimetals. The semimetallic character of GdX introduces additional interaction due to the existence of free electrons. GdN is a ferromagnet with a Curie temperature of T_C=58 K. The neutron diffraction experiments on GdP, GdAs, GdSb, and GdBi suggest that they are antiferromagnets. The Néel temperatures increase from 15.9 to 25.8 K in going from P to Bi. The antiferromagnetic (AFM) phase is unstable against chemical composition and external magnetic field. A small change in the stoichiometry can give rise to the ferromagnetic (FM) phase.[4] An external magnetic field[4] can destroy the AFM state and induce the FM state at low temperature. Magnetism is generally described by the indirect exchange interaction here due to the negligible overlap of the f states. Stoichiometric Gd monopnictides have been proposed to be self-trapped magnetic polaron[5,6] materials. A detailed electronic structure is required to obtain a thorough knowledge about the intriguing properties of GdX.

Self-consistent band structure calculations on GdN, GdP, GdAs, and GdSb have been reported[7,8] within the local spin density approximation (LSDA). The 4f states were treated as localized core-like states with fixed spin occupancies. This calculation does not provide the exact positions of the 4f states as obtained from the experimental X-ray photoemission spectroscopy (XPS) and X-ray Bremsstrahlung Isochromat spectroscopy (BIS) results.[9] However, Petukhov *et al.*[8] pointed out that the inclusion of the 4f states in self-consistent calculations affects other band states. The optical conductivity spectrum or any other spectral function needs a very rigorous treatment of the band states and, hence, calculations that go beyond the frozen core treatment are required for the 4f electrons. In order to minimize the error in calculating the optical properties, one needs to treat the 4f states as band states. The spin-spin exchange splitting of the 4f states in the LSDA scheme does not yield the proper positions and separation of the 4f bands. This suggests that additional corrections such as the correlations among the 4f states (LDA+U) should be taken into account in the conventional LSDA. LDA+U (Ref. 10) is a realistic method of handling the on-site Coulomb interactions among the 4f electrons. Such an approach has led to excellent agreement with the magneto-optical experiments in CeSb and CeTe,[11] Pr monopnictides,[12] Nd monochalcogenides,[13] and Tm monochalcogenides.[14] Also the electronic structure of the Eu monochalcogenides has been described satisfactorily by including the correlation effects of the d states along with the f states.[15] In a recent work, the use of the LDA+U method augmented with a rigid shift of the 5d states[16] of Gd led to semiconducting GdN. However, the electronic structure of GdN is still controversial and it is yet to be established definitely through experiments. In order to obtain the correct electronic structure and to include the effect of the 4f states on the optical properties, one must consider these 4f states as band states but screened by an effective Coulomb parameter, U.

Experiments[17,18] provide evidence that low carrier-density materials usually exhibit a minimum in their optical conductivity spectrum and plasma edge in the reflectivity spectrum. A resonance between the plasmons (charge density waves due to the free electron gas) and the incident electromagnetic radiation (light) occurs at a particular frequency, namely the plasma resonance frequency. This interaction leads to the damping of the charge density waves, which in turn leads to the fall of reflectivity and optical conductivity. Light with higher frequency will be allowed to propagate through the medium and will lead to optical transition if the initial and final states exist with such an energy difference. But plasma resonance[19–22] alone cannot suffice for the large resonant

TABLE I. Table contains a, the lattice parameter, muffin-tin radii of Gd, S_{Gd} and pnictogen, S_X, the density of states at the Fermi level (S_I), $N_{S_I}(E_F)$ and the density of states at the Fermi level (S_{II}) with shifts in the 5d and 4f Hubbard bands in Gd, $N_{S_{II}}(E_F)$.

	a (a.u.)	S_{Gd} (a.u.)	S_X (a.u.)	$N_{S_I}(E_F)$ (St./eV)	$N_{S_{II}}(E_F)$ (St./eV)
GdN	9.447	2.739	1.984	0.04	0.00
GdP	10.808	2.864	2.540	0.21	0.15
GdAs	11.042	2.926	2.595	0.22	0.15
GdSb	11.753	2.997	2.879	0.30	0.25
GdBi	11.926	3.041	2.922	0.31	0.30

magneto-optical (MO) Kerr effect observed in some metallic systems. A sharp fall in the reflectivity at the plasma resonance energy immediately followed by a moderately large and sudden interband transition indicates a possible observation of large MO signals. A sharp fall in the reflectivity spectrum of GdP and GdSb (Refs. 5 and 23) indicates that these are compounds likely to show a moderate MO Kerr effect (MOKE). An experimental MOKE investigation is highly relevant in order to shed light on the electronic and magnetic structure of GdX. Since the experimental results of the MOKE on GdX are not available, our work focuses on the comparison of the results of our calculations with the experimental reflectivity spectra and a possible prediction of the MO Kerr spectrum, especially of ferromagnetic GdN, thereupon. Very recent calculations on some rare earth compounds based on the rigid shifts of the 5d (Ref. 16) and 4f bands (Ref. 24) provide better agreement with experimental results. What happens if such shifts are applied in the Gd monopnictides? And more crucially, how is the MOKE spectrum modified if the electronic structure of GdN is changed from semimetallic to semiconducting by applying these rigid shifts? These are the basic questions to which we seek answers in this work.

II. CALCULATIONAL DETAILS

Full potential (FP) self-consistent spin-polarized band structure calculations have been performed for the FM phase of Gd monopnictides by the linear muffin-tin orbital method[25] (LMTO) using the FP-LMTO code developed by Savrasov *et al.*[26] In the LDA+U method,[10] the LDA energy functional is simplified by removing the LDA f-f interactions and adding the strong on-site Coulomb interactions among the f electrons. The computational detail is mentioned in our earlier paper.[12] In LDA+U calculations, the values of U have been estimated from the energy separation of occupied and unoccupied 4f states in XPS and BIS results.[9] The value of the Coulomb parameter U is chosen to be 10 eV for all but GdBi, 12 eV. This set of calculations is denoted by S_I hereafter. Another set of calculations, S_{II}, were performed considering U among the 4f states to be 6 eV. In addition, the 5d and 4f bands of Gd were given rigid shifts. The lower and the upper 4f Hubbard bands are shifted by 2 eV towards E_F and 6 eV away from E_F, respectively. This amounts to an effective U of $6+(6-2)=10$ eV. This has been done with the sole aim of reproducing the results of XPS and BIS.[9] The governing magnetic exchange mechanism[27,28] in these compounds is the d-f Coulomb exchange interaction. The strong on-site Coulomb interaction of the 4f electrons modifies the electronic structure but fails to incorporate the effect on the 5d electrons, which should be there due to the d-f exchange interaction. This effect is brought about by the shifting of the 5d states by 4 eV away from the Fermi level, and should lead us to the correct electronic structure. The values of other Slater integrals F^2, F^4 for the d electrons and F^2, F^4, F^6 for the f electrons used are 0.8 times of their atomic values evaluated within Hartree-Fock (HF) approximation[29] in order to calculate the Coulomb and exchange matrices $U_{mm'}$ and $J_{mm'}$. The experimental lattice parameters with a rock-salt type structure at ambient conditions for all the GdX are given in Table I. The LMTO basis consists of Gd: 6s, 5p, 5d, 4f and pnictogen: (n)s, (n)p, and (n)d, where n refers to the principal quantum number. Charge density, density of states, and the momentum matrix elements were calculated on a grid of 242 **k** points in irreducible Brillouin zone and the **k** space integration was performed using the tetrahedron method. We started the self-consistent calculations treating the Gd ion as trivalent, implying that $4f^7$ electrons are considered to be occupied. In the present paper, we report the ferromagnetic results only due to very low Néel temperatures of Gd(P, As, Sb, Bi).

III. RESULTS AND DISCUSSIONS

The full-potential spin-polarized band structure of GdN for S_I set calculation is depicted in Fig. 1(a). The occupied 4f bands of Gd lie almost 10 eV below the Fermi level, E_F. These are followed by the fully occupied p bands of nitrogen. However, these bands strongly hybridize with the d bands of Gd. At the Fermi level, there is a small overlap of the conduction and the valence bands along $\Gamma-\mathrm{X}$ direction. The spin-polarized band structure shows that there is a small gap in the spin-down channel. This renders a half-metallic nature to GdN, unlike the small-gap insulating state found earlier[7] in the paramagnetic phase. However, the ferromagnetic calculations[8] of GdN later yielded a zero-gap overlap, consistent with our results. The recent SIC-LSD calculation on GdN also yields a half-metallic behavior.[30] The conduction band consists of the unoccupied $4f^7$ states at about 3 eV above E_F, followed by the 5d states of Gd. The spin-

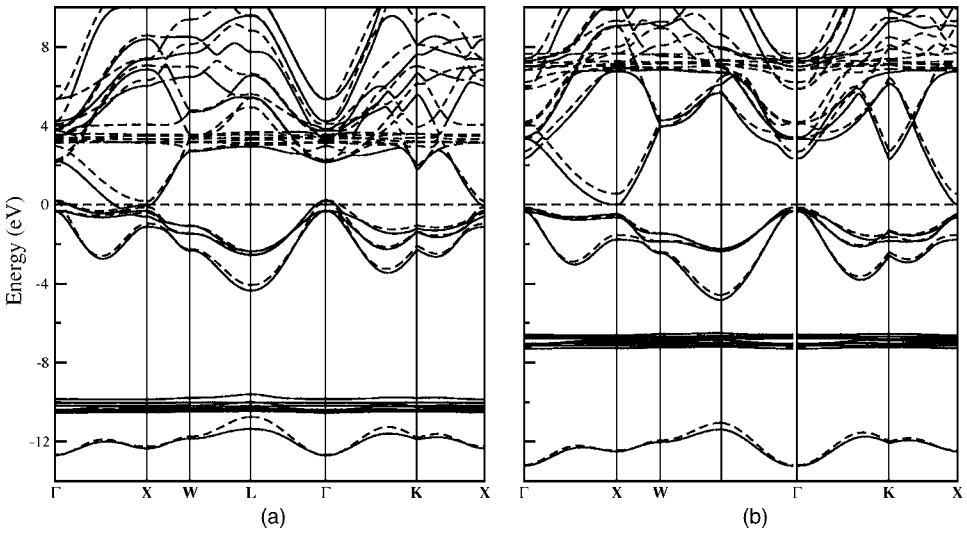

FIG. 1. The band structure of GdN: (a) LDA+U calculations (S_I); (b) LDA+U with rigid shifts of 5d and 4f states of Gd (S_{II}).

polarized band structures of other pnictides are substantially similar to GdN except for the region near E_F, the splitting and the width of the valence p bands and the order of the s bands of the pnictogen. The energy band structure of GdBi is shown in Fig. 2(a). The pnictogen p states show increased spin-orbit (SO) splitting as we go on to the higher pnictogen. Increasing SO interaction leads to increased p-f-d hybridization as we move on from GdP to GdBi. The unoccupied 5d band becomes narrower and moves closer to E_F. The systematic changes in the electronic structure of the series GdX arise from an increase of the lattice parameter and the characteristic trend of the p states due to the increase of the pnictogen ion size.

Experimental XPS and BIS (Ref. 9) indicate that the occupied 4f levels are about 9 eV below E_F and the unoccupied 4f states are about 5 eV above E_F. The energy differences ($\sim$14 eV) between the occupied and the unoccupied f states for $U=10$ eV are in good agreement with the experimental ones in GdP, GdAs, and GdSb. The systematic change of the energy position, though not their actual positions, of the f states are also consistent with the experimental results. In the case of GdBi, the electronic structure with $U=12$ eV was found to be better described than for $U=10$ eV. This gave a peak energy difference between the lower and upper Hubbard bands at just a little above 14 eV. The position of the p valence band of pnictogen in XPS spectra [see Fig. 4 in Ref. 9] is comparable with the theoretical spectra. The only disagreement is in the position of the unoccupied f states relative to E_F. Experimentally, it is about 4–6 eV above E_F and shifts towards E_F from GdP to GdBi. In this set of calculations, it is observed that the bands crossing the Fermi level are 5d (Gd)-p(X) hybridized ones. Secondly, the upper 4f Hubbard band is 2 eV lower in energy in GdP as compared to what has been found in BIS. These two observations motivated us to rigidly shift the 5d states and the 4f Hubbard bands. However, the shift for the 4f states was decided by the difference in the energies of the upper 4f Hubbard band between the previous set of the band structure calculation and the BIS. Figure 1(b) shows the band structure of GdN with $U=6$ eV and the rigid shifts in the 5d and 4f states of the amount stated above. This leads to a decrease in the p-d overlap at E_F and an opening up of a gap in both spin channels in GdN. The band gap may be tuned by suitably choosing the 5d shift parameter. However, in all the other GdX, a shift in the 5d states fails to open up a gap. This is because of the presence of pnictogen p states at the top of the

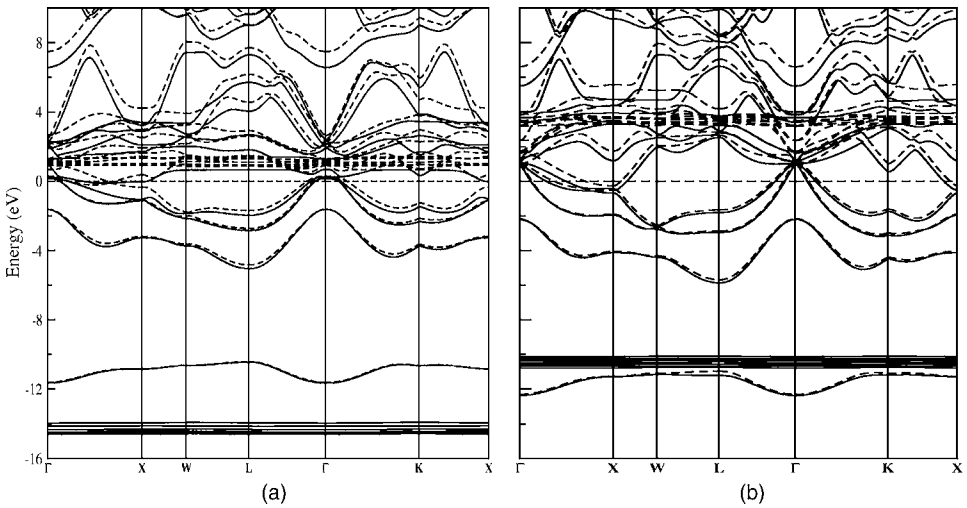

FIG. 2. The band structure of GdBi: (a) LDA+U calculations (S_I); (b) LDA+U with rigid shifts of 5d and 4f states of Gd (S_{II}).

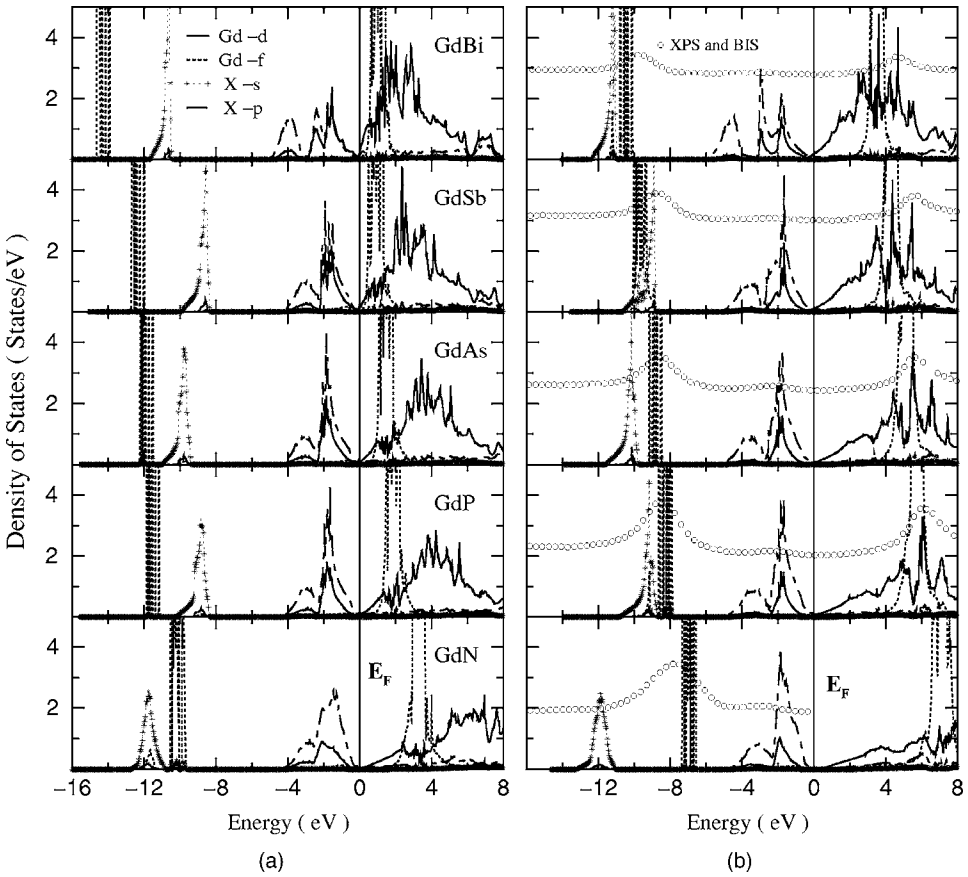

FIG. 3. The *l*-projected density of states of Gd*X* (*X* =N,P,As,Sb,Bi): (a) LDA+*U* calculations (S_I); (b) LDA+*U* with rigid shifts of the 5*d* and 4*f* states of Gd (S_{II}). Experimental XPS and BIS spectra (see Refs. 9 and 34) for the 4*f* states of Gd.

valence band and the bottom of the conduction band too. Figure 2(b) shows the band structure of GdBi with improved positions of the 4*f* Hubbard bands in the new scheme.

Figure 3 shows the angular momentum-decomposed density of states (DOS) of all the Gd monopnictides in the two schemes, left panel for S_I and right panel for S_{II}. Let us first discuss the left panel, i.e., Fig. 3(a). The lowest states are the *s* band of pnictogen in GdN while it appears above the *f* bands for other pnictogens. The separation between the occupied and unoccupied 4*f* bands is almost the same for all Gd*X*. The only change is that the occupied *f* states move away from E_F while the unoccupied *f* states shift towards E_F. The *p* bands of GdN show a broad peak below E_F. The position of the unoccupied 5*d* bands shifts with respect to E_F. Majority states near E_F are the pnictogen *p* states. The total DOS at E_F of GdN, as shown in Table I, is substantially smaller than that of others. This suggests that GdN might be sitting on the fence between semiconducting and semimetallic behavior. The DOS at E_F increases systematically with an increase of the atomic number of pnictogen, though all of them are low-carrier density materials. The calculated DOS with rigid shifts in the 4*f* and 5*d* states as depicted in Fig. 3(b) places the lower 4*f* Hubbard band at 8.25–10.5 eV (7 eV) below E_F in the Gd monopnictides (GdN). But a major improvement is observed in the upper 4*f* Hubbard band which lies 3.5–5.5 eV (7 eV) above E_F in the respective Gd monopnictides (GdN). The better agreement with the BIS is brought about by the shifts in the 4*f* states.

The information on the spin and orbital moment due to each atom and total magnetic moment in all the Gd monopnictides as obtained from both the sets of calculations are given in Table II. In the first set of calculations, the pnictogen

TABLE II. Table contains m_o and m_s, the atomic orbital and spin moments, respectively, and the total moment, m_s+m_o.

	S_I					S_{II}				
	m_s(Gd) (μ_B)	$m_s(X)$ (μ_B)	m_o(Gd) (μ_B)	$m_o(X)$ (μ_B)	m_s+m_o (μ_B)	m_s(Gd) (μ_B)	$m_s(X)$ (μ_B)	m_o(Gd) (μ_B)	$m_o(X)$ (μ_B)	m_s+m_o (μ_B)
GdN	6.79	−0.14	0.13	0.00	6.78	6.99	−0.08	0.01	0.00	6.92
GdP	6.77	−0.12	0.14	0.00	6.79	7.00	−0.06	0.01	0.00	6.95
GdAs	6.77	−0.10	0.15	0.00	6.82	7.01	−0.05	0.01	0.00	6.97
GdSb	6.76	−0.10	0.17	0.00	6.83	7.02	−0.05	0.01	0.00	6.98
GdBi	6.84	−0.10	0.13	0.00	6.87	7.03	−0.05	0.00	0.00	6.99

moment for all the compounds is opposite to the Gd ion. The spin moment due to the polarization of the 4*f* electrons of Gd is 6.64 μ_B. One would have expected a spin moment of 7 μ_B in Gd from its half-filled 4*f* atomic configuration. One would have also expected, from Hund's rule, that the orbital moment would be zero. The $U=10$ eV (12 eV in GdBi) among the 4*f* states fails to quench the orbital moment fully, as can be seen from Table II. Rigid shifts in the 4*f* Hubbard and the 5*d* states yield a spin moment very close to its atomic analog and a fully quenched orbital moment. This is seen clearly for all the Gd*X* in Table II.

Summarizing, it is found that the first set of calculations leads to semimetallic Gd*X*, lower energy position of upper 4*f* Hubbard band, spin moment less than 7.0 μ_B, and not a fully quenched orbital moment. The S_I calculations induce more spin splitting of the *p* states of pnictogen. The combined shifts of the 5*d* and 4*f* states of Gd reduce the antiparallel spin moment of the *p* states. A strong hybridization between the *p* (X) and *d* (Gd) states in the occupied bands is evident. The 5*d* occupation is about 0.7. These support the indirect exchange mechanism for the formation of magnetic state. Lambrecht,[16] assuming that the quasiparticle correction scales inversely with the dielectric constant, has shown that a rigid shift of the 5*d* states of Gd in GdN leads to a formation of energy gap of about 0.8 eV. In our calculations on Eu monochalcogenides,[15] it was found that the inclusion of the Coulomb interactions among the 5*d* states of Eu leads to a gap opening up and simultaneously to a better description of the band structure. The model Hamiltonian calculation on EuO, where the correlation between the localized moments and conduction electrons is represented by an intra-atomic exchange interaction, led to the better electronic structure.[31] The present results also lead to maximum agreement with XPS and BIS measurements and magnetic properties.

The optical conductivity tensor has been calculated from the standard relations given by Reim *et al.*[32] The imaginary component of diagonal optical conductivity (σ^2_{xx}) and the real component of off-diagonal conductivity (σ^1_{xy}) have been calculated using the Kramers–Kronig transformation. The magneto-optical Kerr rotation is calculated from the relation

$$\Phi_k = \theta_k(\omega) + i\epsilon_k(\omega) \approx \frac{-\sigma_{xy}}{\sigma_{xx}\sqrt{1+\frac{4\pi i}{\omega}\sigma_{xx}}}, \qquad (1)$$

where σ_{xx} and σ_{xy} are the diagonal and off-diagonal components of the optical conductivity tensor, provided both are small and $|\sigma_{xy}| \ll |\sigma_{xx}|$. Here θ_k and ϵ_k are the Kerr rotation and the Kerr ellipticity, respectively. Optical and magneto-optical spectra have been calculated for all the Gd*X* using the LMTO band structure and further, a Lorentzian broadening of about 0.0136 eV has been used in order to obtain the best agreement with the experimental results of GdSb and GdAs. Optical conductivity calculations have been performed up to 30 eV for maximum accuracy in calculating $\sigma^2_{xx}(\omega)$ and $\sigma^1_{xy}(\omega)$.

Figure 4 shows the real part of the diagonal conductivity σ^1_{xx} for the Gd*X* with S_I and S_{II} sets of calculations. The optical conductivity spectrum of GdN is quite different from

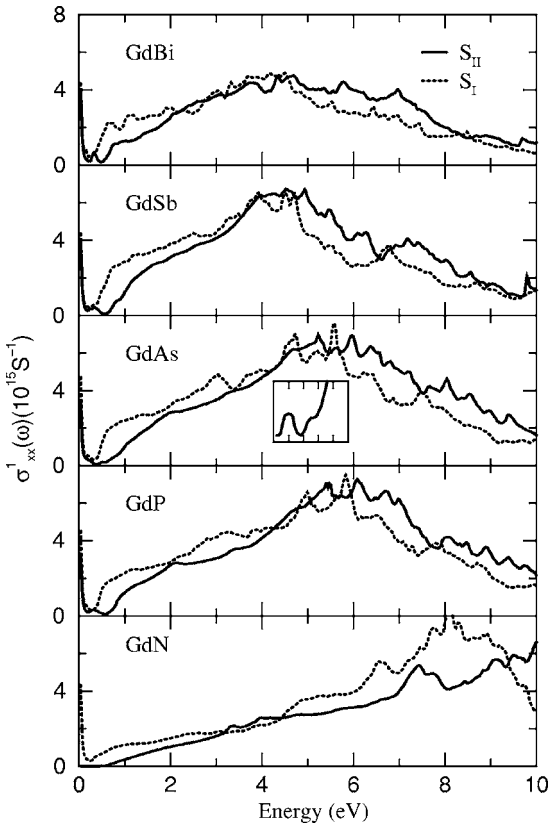

FIG. 4. The real component of the diagonal optical conductivity. The inset shows on enlarged scale in the low energy (upto 1 eV) regime for GdAs.

other pnictides in the S_{II} calculations. The main features in GdN are a double structure between 3 and 4 eV and a major structure at about 7 eV. The former is due to transitions from the N *p* states to the Gd 5*d* states. The peak at 7 eV is caused by a transition from the strongly localized 4*f* lower Hubbard band to the 5*d* states of Gd. This peak occurs in the background of the continuous nitrogen *p* to the Gd 5*d* states transitions, which start from about 0.85 eV. It is worthwhile to remember that the excitonic effects will complicate matters at the absorption edge near 0.6 eV and might lead to a redefinition of the spectrum above 0.6 eV.

All the other Gd*X* show a small interband transition at about 0.33, 0.18, 0.33, and 0.33 eV with an increasing pnictogen size. The Drude contribution suppresses this structure but cannot wipe it out except in GdAs. For GdP and GdSb, the experimental optical conductivity has not been reported yet. However, the imaginary component of the dielectric function spectra of the two[5,23] imply that the corresponding optical conductivity will show a structure near 0.5 and 0.25 eV in GdP and GdSb, respectively. Hence, there is a fair amount of agreement as far as GdP and GdSb are concerned. The experimental diagonal conductivity spectrum of GdAs (Ref. 6) shows two very distinct features. One is at about 0.1 eV and the other is at 0.4 eV. The former is said to be proportional to the number of effective carriers and the latter owes its existence to the self-trapped magnetic polaron effect. On comparing with our S_{II} calculations, we find that the first experimental structure corresponds to the one at 0.18 eV

in the calculated spectrum. Not the $4f$ but the X p and Gd $5d$ electrons have a direct influence over this structure. This is very unlike the light rare earth compounds where the low energy optics are governed by the f electrons. From GdP to GdBi, the first structure occurs at 0.33 eV in all semimetallic GdX but GdAs in the S_{II} calculations. This decrease in the energy of the first interband transition in GdAs is curiously observed in both the experimental and calculated results. A more detailed experimental investigation and rigorous theoretical calculations are necessary in order to understand this unique feature in GdAs. The Drude minimum occurs at a slightly higher energy of about 0.55, 0.36, 0.55, and 0.48 eV from GdP to GdBi. Transitions from the X p to Gd $5d$ states start immediately following the minimum and give rise to the shoulder effect. The largest peak due to this transition occurs at 6, 5, 4.5, and 4.3 eV from GdP to GdBi. This decreasing feature, quite common in the RE monopnictides, is due to the shrinking of the $5d$ conduction bands towards E_F. The transitions from the lower $4f$ Hubbard band occur at energies $\geqslant$10 eV and those to the upper $4f$ Hubbard band from the occupied Gd $5d$ bands peak at about 9, 8, 7, 6, and 6 eV from GdN to GdBi. However, the structure due to the $p \rightarrow d$ and $d \rightarrow f$ transitions occur at almost the same energy range, making it very difficult to distinguish between them. Sharp distinctions are also observed in two sets of calculations especially at low and high energy regions. Strong interband transitions among the p-d hybridized bands are moved to higher energies when the $5d$ bands are shifted. The small structure at low energy is missing when the $5d$ band is not shifted.

The reflectivity spectra for all the GdX for the S_{II} calculations have been depicted in Fig. 5 and compared with the experimental spectrum of that of GdAs and GdSb. Also a comparison with S_I calculations in GdN and GdSb has been made. The S_{II} spectra indicate the deep minimum at a lower energy except in GdN. A structure at around 0.7 eV is due to the p to d transitions. This edge effect takes place at 0.49, 0.435, 0.51, and 0.49 eV in the semimetallic GdX with an increasing atomic number of X. This region is marked by a sharp dip in reflectivity, immediately followed by an equally sharp rise. The sharp rise, with a shoulder like effect, is due the X p to $5d$ transitions. The structure at the lower energy in the conductivity spectrum, which could not be suppressed by the Drude contribution appears as a very fine structure in the reflectivity spectrum in GdAs, GdSb, and GdBi. The first structure in GdP beyond the reflectivity minimum in S_{II} calculations agrees fairly well with the experimental one.[23] The strongest peak appears at about 1.0 eV compared to the experimental value of 1.4 eV for $GdP_{0.994}$. Guntherodt *et al.* pointed out that the stoichiometry and the fluorine content may perturb the experimental results strongly. And of course the experimental results at 300 K imply that a large thermal broadening effect makes the structure more flat. These two points might account for the small discrepancy between the calculated and experimental spectra. However, the position of the reflectivity minima of GdAs and GdSb tally satisfactorily with the more recent experimental counterpart,[5,33] which are performed respectively at 6 and 15 K. The edge effect is made distinct by the shoulder which arises due to the transition from the p bands of pnictogen to the $5d$ conduction bands of Gd. The double structure, very prominent in the experimental spectrum, is also found in the theoretical spectrum. This structure reflects the effect of spin-orbit splitting of the Sb p states.

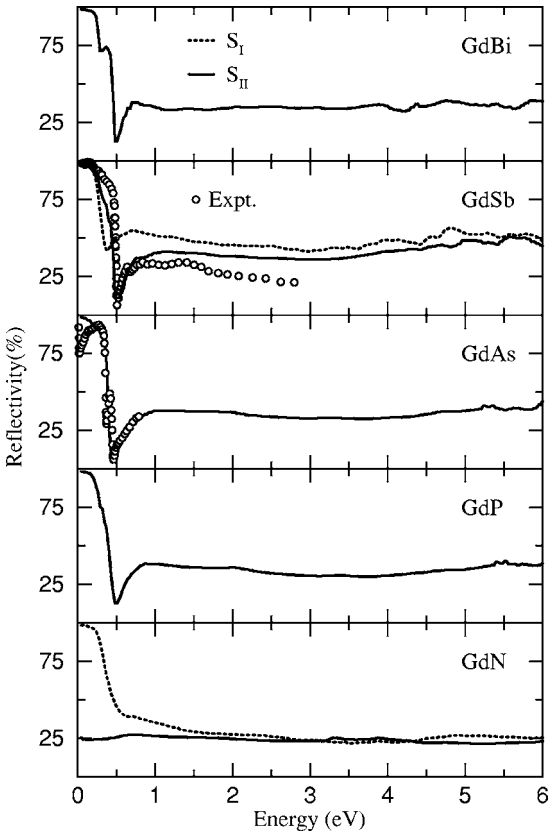

FIG. 5. The calculated reflectivity spectra of the Gd monopnictides and the experimental reflectivity spectra of GdAs (see Ref. 33) and GdSb (see Ref. 5).

The real ϵ^1_{xx} and imaginary ϵ^2_{xx} parts of the dielectric tensor calculated within S_{II} are shown in Fig. 6. The real ϵ^1_{xx} spectrum gives the coupled plasma resonance energy where it assumes the value 0. Table III contains the calculated bare plasma frequency ω^b_{pl}(cal) obtained from the LMTO band structure and the screened plasma resonance frequency, ω^{scr}_{pl}(cal) estimated from the real component of the dielectric function for the two sets of calculations. The theoretical values of the screened and bare plasma frequency of GdP are in close agreement with the experimental ones of 0.52 and 1.53 eV for $GdP_{0.994}$, respectively.[23] The value of ϵ^1_{xx} increases steeply near the energy axis. The imaginary ϵ^2_{xx} decreases sharply at low energies to a minimum value. The dielectric function spectrum of GdP at low energy is similar in nature to that of the experimental one[23] in $GdP_{0.994}$. A close look at the experimental spectrum provides support to the small structure we observe just below the minimum in the optical conductivity and reflectivity spectra for GdP. A prominent peak in the calculated ϵ^2_{xx} is centered at about 1.0 eV.

Figure 7 shows the complex MO Kerr rotation spectra (S_{II}) for GdX. Ferromagnetic GdN exhibits a MO signal of about 0.65° at about 0.85 eV and is due to the nitrogen

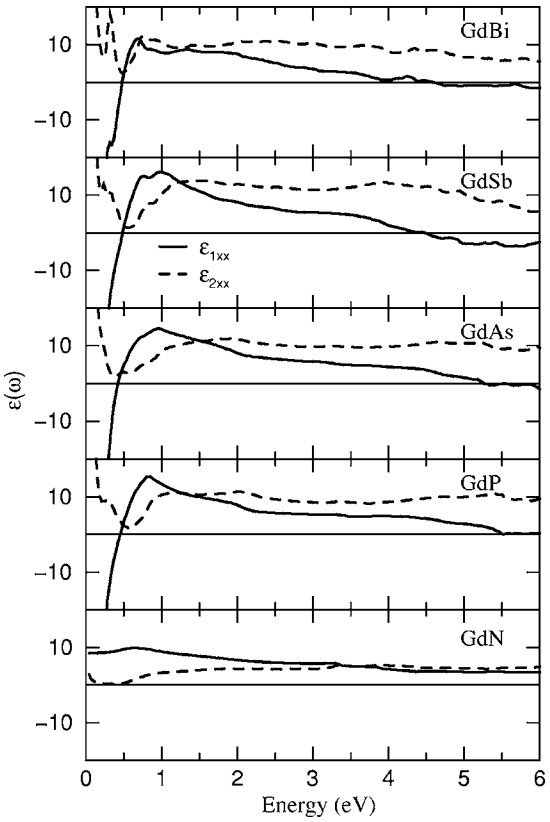

FIG. 6. Real and imaginary components of ϵ_{xx}.

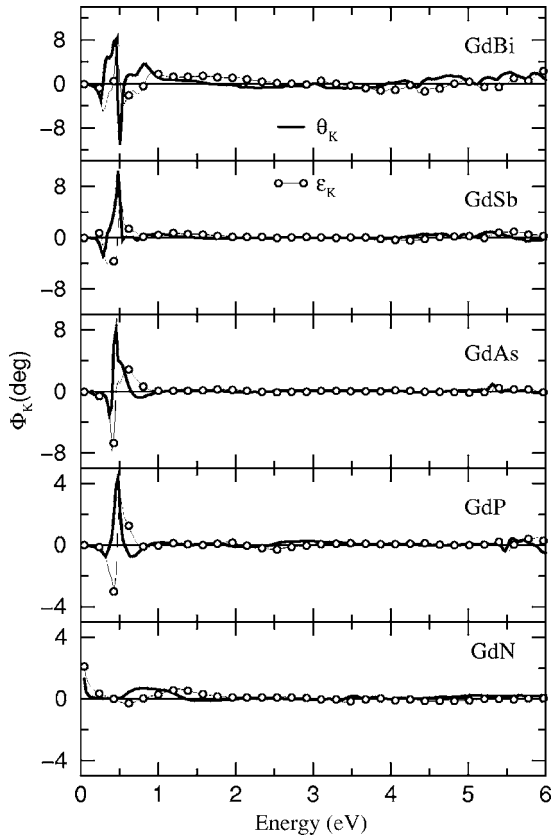

FIG. 7. The calculated complex Kerr spectrum of GdX, θ_K, Kerr rotation, and ϵ_K, Kerr ellipticity.

$p \rightarrow$ Gd d bands transition. The Kerr rotation spectrum shows a large positive rotation of approximately 8° in GdP, GdAs, and GdSb, and a double rotation in GdBi in the low energy region. Sharp resonances can be observed in all but GdN. The largest positive Kerr rotation of about 10.6° is found in GdSb at 0.478 eV, with a width of ~0.192 eV. At this energy, the diagonal conductivity (both the real and imaginary components) assumes a minimum value. The real component is minimum at the Drude minimum (0.55 eV) and the imaginary component is minimum at the plasma resonance energy (0.48 eV). However, the off-diagonal conductivity, though small, is almost without any characteristic feature. The rotation is basically due to the nonzero off-diagonal conductivity and the simultaneously minimum value of the diagonal conductivity. Hence, we find that there is a strong correspondence between the plasma resonance, the plasma edge, and the Kerr rotation in all the semimetallic GdX. The absolute value and the narrowness of the peak increase from GdP to GdSb. In GdBi, multiple structures are found implying strong spin-orbit coupling. The trend in the absolute value of the rotation is commensurate with the depth of the plasma minima. The ellipticity as a function of the energy also exhibits a sharp structure at the plasma resonance frequency along the series. The resonance in ellipticity takes place between 0.44 and 0.5 eV in GdSb. The $4f$ to $5d$ transitions occur at energies $\geqslant$10 eV. And there is no sizable MO signal due to such a transition. There are no experimental or theoretical reports of MO Kerr rotation in GdX. Hence, it will be worthwhile to perform MOKE experiments on Gd monopnictides in order to ascertain the influence of the $4f$ electrons on high-energy optical properties of GdX.

TABLE III. The table contains the bare plasma frequency, ω_{pl}^{b} and the screened plasma frequency, ω_{pl}^{scr} for S_I and S_{II}.

	S_I		S_{II}	
	ω_{pl}^{b} (eV)	ω_{pl}^{scr} (eV)	ω_{pl}^{b} (eV)	ω_{pl}^{scr} (eV)
GdP	1.76	0.35	1.55	0.45
GdAs	1.69	0.35	1.66	0.42
GdSb	1.32	0.33	2.12	0.48
GdBi	1.27	0.28	2.36	0.48

The energy loss spectrum is shown in Fig. 8 for S_{II}. A sharp energy loss peak is seen at the plasma resonance energies of which the largest one is that for GdSb.

The polar Kerr rotation spectrum follows the off-diagonal conductivity spectrum σ_{xy} since the latter carries all the information regarding the spin polarization, spin-orbit interaction, and the coupling between the two. In light rare earth compounds,[17,18] the largest Kerr rotation is attributed to the $f \rightarrow d$ transitions which produce sharp peaks in σ_{xy}. The broad peaks between 0.5 and 2 eV in GdX proves the absence of the $f \rightarrow d$ transitions at such an energy. As the $4f$ level lies fairly deep in the valence band, the $f \rightarrow d$ transition is not responsible for the large Kerr rotation at low energy in GdX. The negligible orbital moment also indicates that it

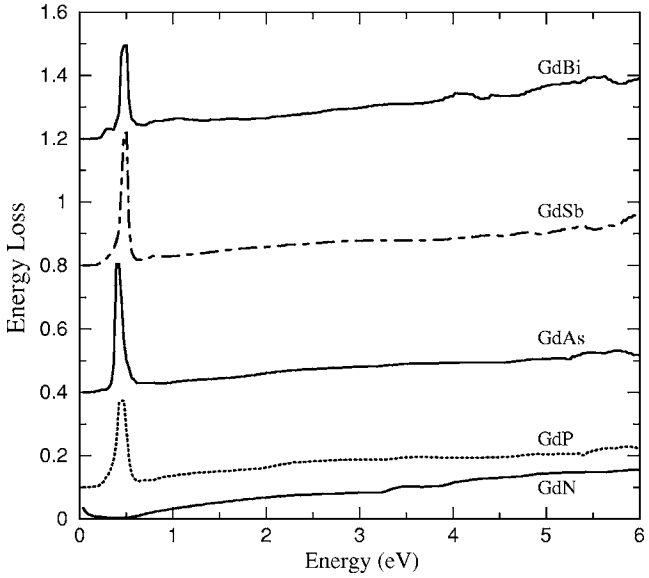

FIG. 8. The calculated energy loss spectrum of GdX. For the sake of visibility the spectra of GdP, GdAs, GdSb, and GdBi are shifted upwards by 0.1, 0.4, 0.8, and 1.2 units, respectively.

cannot contribute singularly to the Kerr effect. The plasma resonance effect is one of the most important factors in the Kerr rotation phenomenon. The present theoretical calculations indicate that the enhanced magneto-optical Kerr rotation is associated with the low value of reflectivity $\approx 11\%$, i.e., the plasma minimum and the pronounced plasma edge effect near $\epsilon_{xx}^{1} \approx 0$ in GdX. For the low-energy optical properties, the plasma resonance effect gives rise to a significant Kerr signal in semimetallic GdX. The magnitude of the Kerr signal may be modified in practice. But within the limitations of one-electron and other approximations, we have been able to predict a reasonable Kerr spectrum for Gd monopnictides.

Calculations performed with the 4f electrons frozen in the core lead to an increase in carrier concentration. The increase in the DOS at E_F is evident in GdN too. The pnictogen p bands and the Gd 5d bands are modified. This leads to an increase in the bare plasma frequency. The reflectivity minimum loses its sharpness and shows a substantial deviation from experiment. The edge effect or shoulder loses its prominence. The spin-spin exchange splitting in X p electrons and the Gd 5d electrons is absent since the 4f electrons are now frozen in the core. This leads to an almost non-existent off-diagonal conductivity and Kerr spectra in all the GdX. Hence, the frozen core treatment of the 4f electrons does not provide the optical and magneto-optical properties of GdX.

The uncertainty in the position of the unoccupied 4f bands remains due to the unavailability of the experimental BIS and optical data of GdN. The XPS and BIS of the elemental Gd implies that the unoccupied 4f level in the elemental Gd lies at about 4 eV above the Fermi level. And recent XPS data[34] of GdN show the energetics of the occupied 4f levels comparable to that of metallic Gd. In order to investigate the effect of the 4f position on the electronic and magnetic properties of GdN, calculations have been carried out by appropriate shifting of the upper Hubbard band to place the unoccupied 4f position similar to the elemental Gd, as shown in Fig. 9. No appreciable changes occur in the vicinity of the Fermi level. The hybridization of the 4f states results in small changes in the spin splitting of the p states of nitrogen. As a result, the net moment reduces by a small amount to 6.89 μ_B. The position of the unoccupied 4f bands varied between 4 and 8 eV above E_F in the calculations does not influence the electronic and magnetic properties significantly. As far as the optical properties are concerned, the high-energy structures due to the 5d to 4f upper Hubbard band transitions quite expectedly shift towards lower energy values. However, the low-energy optical spectra remain almost unchanged. Much more experimental investigations are necessary in order to get a thorough idea about the physical properties of GdN.

The strongly correlated f states in the Gd monopnictides create a very complicated issue in explaining the electronic structure and magnetic properties. The on site Coulomb interaction arising from the localized character of the 4f shells

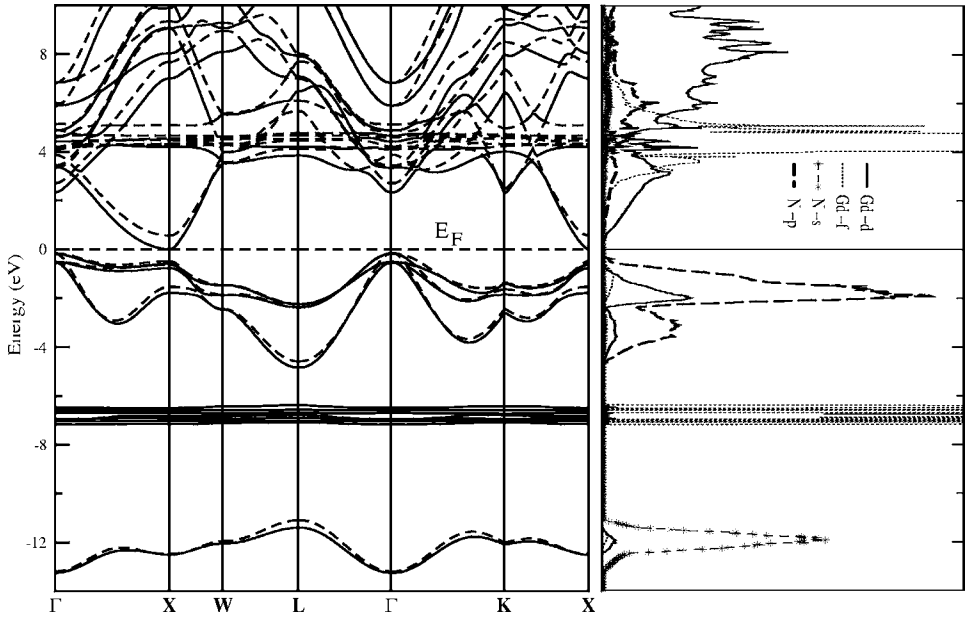

FIG. 9. LDA+U energy band structure and density of states of GdN, as that of S_{II}, but calculated with an auxuliary shift of 1.5 eV to the 4f states.

is taken into account in the LDA+U scheme. The *ab initio* electronic structure calculation using the values of U estimated from the experimental XPS and BIS results[9] leads to the occupied 4f bands well below E_F and the unoccupied bands nearer to E_F. Hence, the LDA+U technique does not reveal the experimental positions of the 4f bands. The orbital degrees of freedom are not allowed due to the half filling of the 4f shell in Gd. The additional self-interaction term in the LDA+U Hamiltonian is essential to obtain the correct positions of the 4f states. For this purpose, rigid shifts in lower and upper Hubbard bands are performed in an approximate way to consider the proper self-energy correction of the 4f states. The amount of shifts as mentioned in Sec. II gives rise to the 4f positions in good agreement with the experiments. One of the controversial problems in GdN is the existence of a semiconducting or semimetallic ground state at the exact chemical composition. The single degenerate 5d state derived from 5d t_{2g} at the Γ point of the Brillouin zone overlaps with the 2p level of N near the X point. The reasonably wide 5d band restricts the inclusion of U in the self-consistent calculations. The electronic structure has been modified by shifting the 5d bands upwards and consequently generates a band gap. The LDA calculation underestimates the gap while the GW approximation[35] provides good band gaps in the semiconductors. The rigid shift of the 5d states to open a gap may be similar to the self-energy correction in the GW method.

The magnetism of GdX is highly complex to understand the exchange mechanism. The magnetic moment stems from the half filled 4f shell of Gd. The direct exchange interaction among neighboring Gd ions is not possible due to the localized electrons. The 4f moments are mediated via 5d conduction and pnictogen p electrons. The intra-atomic f-d exchange[27,28] coupling plays an important role in such interaction. The strength of d-f interaction depends on the relative energy positions of the p, d, and f bands. In the first set (S_I) of calculation, the spin down unoccupied 4f levels lie close to E_F and are extended more than occupied 4f band due to the strong 4f-4f spin exchange interaction. This contributes to the spin moment. The induced moments in the p states of pnictogen are antiparallel to the 4f moments. The combination of these two opposite moments reduces the net moment to 6.638 μ_B which is low compared to the expected value of 7.0 μ_B. The correct positions of the 4f bands give rise to an improved moment by significantly reducing the magnitude of the spin down channel. The added correction in the 4f states enhances the induced anion moment. The 5d moment is parallel to the local 4f moments according to Hund's rule. The exchange coupling occurs through the p-d interaction. The 5d occupation arises from the p-d hybridization. The upward shifting of the 5d states reduces the spin polarization of both 5d (Gd) and p (X). The spin splitting of the 5d conduction bands and anion valence bands are required for intra-atomic f-d exchange coupling as observed in isostructural EuO.[36] Moreover, the hybridization between the 5d and p states provides the required number of 5d electrons for participating in the f-d interaction. The rigid shifts in the 4f and 5d bands affect these to optimize intersite coupling. The present calculations establish that the magnetic exchange coupling is mediated by small spin polarizations of conduction and valence bands and an appreciable amount of the 5d character of 0.7.

IV. CONCLUSION

A rigid shift of both the 5d and 4f states in the LDA+U potential leads to the semiconducting GdN and exact positions of the 4f states in GdX. The amount of shift in the 5d states of Gd is of the order of the Coulomb correlation parameter in typical 3d/4d transition metal ions. Magnetism is spin exchange driven and is very close to 7 μ_B. The deep minimum in the reflectivity spectra occurs in all the semimetallic GdX. The first interband structure in optical conductivity in GdAs occurs at a lower energy than in the other Gd pnictides. A moderate rotation of 0.65° at 0.85 eV for ferromagnetic and semiconducting GdN and larger rotations for the other Gd monopnictides are predicted. The excitonic and magnetic polaron effects in GdX may modify the Kerr spectra at this energy. However, more experimental data are required to establish a semiconducting nature of GdN and magneto-optical properties of Gd monopnictides.

ACKNOWLEDGMENTS

One of the authors, D.B.G., is thankful to the IFW, Dresden, for the computational facilities. The authors thank Professor S. Kimura and Dr. Frank Leuenberger for providing experimental data and fruitful suggestions. This work is funded by the Department of Science and Technology, Government of India (Project No. SP/S2/M-50/98).

[1] D. X. Li, Y. Haga, H. Shida, T. Suzuki, and Y. S. Kwon, Phys. Rev. B **54**, 10483 (1996).
[2] D. X. Li, Y. Haga, H. Shida, T. Suzuki, Y. S. Kwon, and G. Kubo, J. Phys.: Condens. Matter **9**, 10777 (1997).
[3] T. Tomimatsu, K. Koyama, M. Yoshida, D. Li, and M. Motokawa, Phys. Rev. B **67**, 014406 (2003).
[4] D. X. Li, Y. Haga, H. Shida, T. Suzuki, T. Koide, and G. Kido, Phys. Rev. B **53**, 8473 (1996).
[5] Y. S. Kwon, M. H. Jung, K. R. Lee, S. Kimura, and T. Suzuki, Physica B **240**, 88 (1997).
[6] S. Kimura, D. X. Li, Y. Haga, and T. Suzuki, J. Magn. Magn. Mater. **177–181**, 351 (1998).
[7] A. Hasegawa and A. Yanase, J. Phys. Soc. Jpn. **42**, 492 (1977).
[8] A. G. Petukhov, W. R. L. Lambrecht, and B. Segall, Phys. Rev. B **53**, 4324 (1996).
[9] H. Yamada, T. Fukawa, T. Muro, Y. Tanaka, S. Imada, S. Suga, D. X. Li, and T. Suzuki, J. Phys. Soc. Jpn. **65**, 1000 (1996).
[10] V. I. Anisimov, J. Zaanen, and O. K. Andersen, Phys. Rev. B **44**, 943 (1991); A. I. Liechtenstein, V. I. Anisimov, and J. Zaanen, *ibid.* **52**, R5467 (1995); A. I. Liechtenstein, V. P. Antropov, and

B. N. Harmon, *ibid.* **49**, 10770 (1994); V. I. Anisimov, I. V. Solovyev, M. A. Korotin, M. T. Czyzyk, and G. A. Sawatzky, *ibid.* **48**, 16929 (1993).
[11] D. L. Price, B. R. Cooper, S. P. Lim, and I. Avgin, Phys. Rev. B **61**, 9867 (2000).
[12] D. B. Ghosh, M. De, and S. K. De, Phys. Rev. B **67**, 035118 (2003).
[13] V. N. Antonov, B. N. Harmon, A. Y. Perlov, and A. N. Yaresko, Phys. Rev. B **59**, 14561 (1999).
[14] V. N. Antonov, B. N. Harmon, and A. N. Yaresko, Phys. Rev. B **63**, 205112 (2001).
[15] D. B. Ghosh, M. De, and S. K. De, Phys. Rev. B **70**, 115211 (2004).
[16] W. R. L. Lambrecht, Phys. Rev. B **62**, 13538 (2000).
[17] R. Pittini, J. Schoenes, O. Vogt, and P. Wachter, Phys. Rev. Lett. **77**, 944 (1996).
[18] R. Pittini, J. Schoenes, and P. Wachter, Phys. Rev. B **55**, 7524 (1997).
[19] W. Reim, O. E. Husser, J. Schoenes, E. Kaldis, and P. Wachter, J. Appl. Phys. **55**, 2155 (1984).
[20] H. Feil and C. Haas, Phys. Rev. Lett. **58**, 65 (1987).
[21] F. Salghetti-Drioli, P. Wachter, and L. Degiorgi, Solid State Commun. **109**, 773 (1999).
[22] A. De and A. Puri, J. Appl. Phys. **92**, 5401 (2002).
[23] G. Guntherodt, E. Kaldis, and P. Wachter, Solid State Commun. **15**, 1435 (1974).
[24] V. N. Antonov, B. N. Harmon, and A. N. Yaresko, Phys. Rev. B **69**, 094404 (2004).
[25] O. K. Andersen, Phys. Rev. B **12**, 3060 (1975).
[26] S. Y. Savrasov and D. Y. Savrasov, Phys. Rev. B **46**, 12181 (1992); S. Y. Savrasov, *ibid.* **54**, 16470 (1996).
[27] P. Wachter, Phys. Rep. **44**, 159 (1978).
[28] T. Kasuya and D. X. Li, J. Magn. Magn. Mater. **167**, L1 (1997).
[29] R. D. Cowan, *The Theory of Atomic Structure and Spectra* (University of California Press, Berkley, 1981).
[30] C. M. Aerts, P. Strange, M. Horne, W. M. Temmerman, Z. Szotek, and A. Svane, Phys. Rev. B **69**, 045115 (2004).
[31] R. Schiller and W. Nolting, Phys. Rev. Lett. **86**, 3847 (2001).
[32] W. Reim and J. Schoenes, in *Ferromagnetic Materials*, edited by E. P. Wohlfarth and K. H. J. Buschow (North Holland, Amsterdam, 1990), Vol. 5, p. 133.
[33] S. Kimura, D. X. Li, Y. Haga, and T. Suzuki, Jpn. J. Appl. Phys., Suppl. **11**, 126 (1998).
[34] F. Leuenberger, Ph.D. thesis, Georg-August-Universität Göttingen, 2004; http://webdoc.sub.gwdg.de/diss/2004/leuenberger/leuenberger.pdf.
[35] L. Hedin, Phys. Rev. **139**, A796 (1965); L. Hedin and S. Lundqvist, in *Soild State Physics: Advances in Research and Applications*, edited by F. Seitz, D. Turnbull, and H. Ehrenreich (Academic Press, New York, 1969), Vol. 23, p. 1.
[36] P. G. Steeneken, L. H. Tjeng, I. Elfimov, G. A. Sawatzky, G. Ghiringhelli, N. B. Brookes, and D. J. Huang, Phys. Rev. Lett. **88**, 047201 (2002).